

Production of medical isotopes from a thorium target irradiated by light charged particles up to 70 MeV

This content has been downloaded from IOPscience. Please scroll down to see the full text.

2015 Phys. Med. Biol. 60 931

(<http://iopscience.iop.org/0031-9155/60/3/931>)

View [the table of contents for this issue](#), or go to the [journal homepage](#) for more

Download details:

IP Address: 134.158.27.102

This content was downloaded on 12/01/2015 at 07:57

Please note that [terms and conditions apply](#).

Production of medical isotopes from a thorium target irradiated by light charged particles up to 70 MeV

C Duchemin¹, A Guertin¹, F Haddad^{1,2}, N Michel^{1,2} and V Métivier¹

¹ SUBATECH, Ecole des Mines de Nantes, Université de Nantes, CNRS/IN2P3, Nantes, France

² GIP Arronax, 1 rue Aronnax, 44817 Saint-Herblain, France

E-mail: Charlotte.Duchemin@subatech.in2p3.fr

Received 15 October 2014, revised 5 December 2014

Accepted for publication 12 December 2014

Published 9 January 2015



Abstract

The irradiation of a thorium target by light charged particles (protons and deuterons) leads to the production of several isotopes of medical interest. Direct nuclear reaction allows the production of Protactinium-230 which decays to Uranium-230 the mother nucleus of Thorium-226, a promising isotope for alpha radionuclide therapy. The fission of Thorium-232 produces fragments of interest like Molybdenum-99, Iodine-131 and Cadmium-115g. We focus our study on the production of these isotopes, performing new cross section measurements and calculating production yields. Our new sets of data are compared with the literature and the last version of the TALYS code.

Keywords: thorium, cross-section, stacked-foils, fission, TALYS

(Some figures may appear in colour only in the online journal)

1. Introduction

Nuclear medicine uses radionuclides for both diagnostic and therapeutic purposes. Depending on the radiation emitted by the radioactive isotope, it can be used for one or other application. For diagnosis, with the number of examinations estimated to have been between 25 and 30 million in 2008 with a projected increase rate of 1.5 to 2.5% until 2020 (AIPES 2008), ^{99m}Tc is the most commonly used agent in Single-Photon Emission Computed Tomography (SPECT). Five main reactors provide ⁹⁹Mo, which is the mother nucleus of ^{99m}Tc, for medical applications: NRU in Canada, HFR in Netherlands, SAFARI-1 in South Africa, BR2 in Belgium and OSIRIS in France. All these reactors are ageing and have been suffering from unscheduled

shutdowns since 2009. Both OSIRIS and NRU, which provide 45% of the worldwide production, are expected to stop operating in the near future (2015 and 2016, respectively). This has created a so-called ‘ ^{99m}Tc crisis’ and several international committees are set to tackle this issue. The NEA Steering Committee for Nuclear Energy established the High-Level Group on the Security of Supply of Medical Radioisotopes (HLG-MR) and requested a review of other potential methods for the production of $^{99}\text{Mo}/^{99m}\text{Tc}$ using reactors or accelerators (NEA 2010). Within this framework, cross section data on some alternative production routes are required.

For therapy, there is actually a great interest in alpha emitters. These radionuclides are able to deliver a large dose over a small distance leading to a high linear energy transfer and a high cytotoxic effect. Among them, Astatine-211 (Zalutsky *et al* 1989), Radium-223 (Harrison *et al* 2013), Bismuth-213 (Morgenstern *et al* 2012) and Thorium-226 (Friesen *et al* 2009) have great potential in the therapy of oncologic diseases. Again, in this case, cross section measurements will help to define the best production route giving us the opportunity to make these radionuclides available to the scientific community.

The irradiation of a thorium target by light charged projectiles like protons or deuterons produces alpha emitters by an activation process and ^{99}Mo by fission.

In this paper, new cross section values are presented for the $^{232}\text{Th}(\text{p},\text{x})^{230}\text{Pa}$, ^{227}Th , ^{225}Ac and the $^{232}\text{Th}(\text{d},\text{x})^{230}\text{Pa}$ reactions and for the radioisotopes of medical interest coming from the fission of thorium (^{99}Mo , ^{115g}Cd and ^{131}I) using protons and deuterons as projectiles. Measurements have been made using the ARRONAX cyclotron (Haddad *et al* 2008) up to 70 MeV with protons and up to 34 MeV with deuterons.

These data have been compared with the results of the TALYS code and used to calculate production yields with high accuracy. A special emphasis has been put on the ^{99}Mo production which has been estimated in the past by extrapolating low proton energy data (Abbas *et al* 2012).

2. Materials and methods

2.1. Experimental set-up

With the ARRONAX cyclotron, the cross section measurements are made using the stacked-foils method (Blessing *et al* 1995, Duchemin *et al* 2015) which consists in the irradiation of a set of thin foils, grouped as patterns. Each pattern contains a target (here a thorium foil) to produce the isotopes of interest, a monitor foil to have information on the beam flux and a degrader to change the incident beam energy which impinged the thorium foils. In this work, 40 μm thick thorium targets, 10 or 20 μm thick titanium, nickel and copper monitor foils and thick aluminium and copper degrader foils (between 500 μm and 1 mm) were irradiated.

The ARRONAX cyclotron can deliver proton or deuteron beams with an energy uncertainty within ± 0.50 MeV and 0.25 MeV respectively, as specified by the cyclotron provider using simulations. The beam line was closed using a 75 μm thick kapton foil and the stacks were located about 7 cm downstream in air. The energy through each thin foil was determined in the middle of the thickness of the foil using the SRIM software (Ziegler *et al* 2010). Energy loss in the kapton foil and air were taken into account. All foils were provided by Goodfellow[®] with high purity (>99.5%). The natural isotopic compositions of the foils are reported in table 1.

All along the stack, depending on the number of foils, the energy uncertainty calculated using the SRIM software (Ziegler *et al* 2010) increases up to ± 1.8 MeV due to the energy straggling. Several stacks were irradiated with a different incident energy in order to minimize

Table 1. Purity and isotopic composition of the thin foils purchased from Goodfellow®.

Nature	Purity	Isotopic composition				
Titanium	99.6%	⁴⁶ Ti	⁴⁷ Ti	⁴⁸ Ti	⁴⁹ Ti	⁵⁰ Ti
		8.0%	7.5%	73.7%	5.5%	5.3%
Nickel	99.9%	⁵⁸ Ni	⁶⁰ Ni	⁶¹ Ni	⁶² Ni	⁶⁴ Ni
		68.27%	26.10%	1.13%	3.59%	0.91%
Copper	99.9%	⁶³ Cu	⁶⁵ Cu			
		69.2%	30.8%			
Thorium	99.5%	²³² Th				
		100%				

this energy dispersion and cover the full energy range from 70 MeV down to 11 MeV for protons and from 34 MeV down to 8 MeV for deuterons, which cover the whole energy range of interest. Conducting several experiments using different incident beam energy, we were able to overlap some data points. A good overlap has been obtained, validating the method and the quality of our data and indicating that our experiments are under control. Typical irradiations were carried out with a beam intensity between 100 and 150 nA for 30 min. Irradiation conditions are reported in table 2.

Each thin foil has been weighed before irradiation using an accurate scale ($\pm 10^{-5}$ g) and scanned to precisely determine its area. The thickness is deduced from these values, assuming it is homogeneous over the whole surface. Monitor foils have been placed behind each target foil, to record the particle flux all along the stack through reactions recommended by the International Atomic Energy Agency. For all the experiments using deuterons as projectiles, the recommended cross section of the reaction $^{nat}\text{Ti}(d,x)^{48}\text{V}$ (Tárkányi *et al* 2001) is used because of its availability over the whole studied energy range, between 8 and 34 MeV. In the case of protons as projectiles, different monitor reactions were used, depending on the incident beam energy: $^{nat}\text{Ti}(p,x)^{48}\text{V}$ below 20 MeV, $^{nat}\text{Ni}(p,x)^{57}\text{Ni}$ between 20 and 46 MeV, $^{nat}\text{Cu}(p,x)^{62}\text{Zn}$ from 46 up to 60 MeV and $^{nat}\text{Cu}(p,x)^{56}\text{Co}$ up to 70 MeV (Tárkányi *et al* 1991, Takács *et al* 2002, Tárkányi *et al* 2012, Michel *et al* 1997). A Faraday cup was placed after the stack to collect charges and control the intensity during the irradiation. The cross section values obtained with this measurement are in agreement with the recommended ones, which are within 6% for protons. The activity measurements in each target and monitor foil were performed using a high purity germanium detector from Canberra (France) with low-background lead and copper shielding. All foils were counted twice: starting the day after the irradiation and after 2 or 3 weeks. The foils were counted for a minimum of 24 h (one day) and up to 60 h (during the weekend) depending on the statistics in the peaks of interest. Gamma spectra were recorded in a suitable geometry calibrated in energy and efficiency with standard $^{57,60}\text{Co}$ and ^{152}Eu gamma sources from LEA-CERCA (France). The full widths at half maximum were 1.04 keV at 122 keV (^{57}Co ray) and 1.97 keV at 1332 keV (^{60}Co ray). Samples were placed at a height of 19 cm from the detector in order to reduce the dead time and the effect of sum peaks. The dead time during the counting was always kept below 10%.

2.2. Data processing

The activity values of the produced radioisotopes were derived from the γ spectra and the nuclear decay data given in table 3, using the Fitzpeak spectroscopy software (FitzPeaks Gamma Analysis and Calibration Software Version 3.66).

Table 2. Irradiation conditions and energies estimated with SRIM.

Protons					
Beam energy (MeV)	<Intensity> (nA)	Energy points (MeV)			
70.3 (5)	145	70.12 (53)	57.68 (103)		
46.3 (5)	103	45.92 (56)	41.06 (79)	36.92 (93)	
30.7 (5)	106	30.19 (56)	25.53 (79)	20.08 (107)	
30.7 (5)	103	17.81 (118)	14.38 (141)	11.05 (178)	
Deuterons					
Beam energy (MeV)	<Intensity> (nA)	Energy points (MeV)			
34.00 (25)	109	33.10 (32)	32.00 (37)	31.00 (39)	26.74 (51)
30.75 (25)	106	29.88 (32)	28.33 (38)	25.23 (45)	23.43 (52)
30.75 (25)	141	16.60 (69)	14.33 (81)	11.79 (93)	8.73 (114)
28.70 (25)	51	27.79 (33)	22.98 (46)		
22.59 (25)	97	21.47 (32)	19.61 (39)		

Table 3. Nuclear data associated to the radionuclides of interest (National Nuclear Data Center 0000, Ekström and Firestone 2004).

Radioisotope	$T_{1/2}$	E_{γ} (keV)	I_{γ} (%)	Reaction	$E_{\text{threshold}}$ (MeV)
^{225}Ac	10.0 (1) d	218.19 (^{221}Fr)	11.6 (4)	(p,2p6n)	42.089
				(p,p7n) + decay	43.549
				(d,2p7n)	44.514
				(d,p8n) + decay	45.981
^{227}Th	18.72 (2) d	235.971	12.3 (9)	(p,p5n)	30.848
		256.250	7.0 (4)	(p,6n) + decay	32.663
				(d,p6n)	33.224
				(d,7n) + decay	35.048
^{230}Pa	17.4 (5) d	951.95	29.1 (14)	(p,3n)	13.710
				(d,4n)	16.013
^{99}Mo	65.94 (1) h	181.063	5.99 (7)	(p,f)	
		366.421	1.191 (13)	(d,f)	
		739.500	12.131 (2)		
		777.921	4.26 (5)		
^{115}gCd	53.46 (10) h	260.89	1.94 (1)	(p,f)	
		336.24	45.9 (1)	(d,f)	
		492.30	8.03 (9)		
		527.90	27.45 (18)		
^{131}I	8.0207 (11) d	80.185	2.62 (3)	(p,f)	
		284.305	6.14 (5)	(d,f)	
		364.489	81.7 (6)		
		636.989	7.17 (9)		

Knowing the precise thickness of the foil and the activity value of the produced isotope, its production cross section is calculated using the well-known activation formula (Duchemin *et al* 2015). The isotopic purity of the sample was taken into account. As each target is followed by a monitor foil which receives the same particle flux, the cross section is deduced with a relative calculation using the recommended cross section. The

uncertainty on the production cross section is calculated in a quadratic form (Duchemin *et al* 2015). The main errors come from the measured activity (around 3% for fission products, up to 15% for ^{230}Pa and ^{227}Th and around 20% for ^{225}Ac), the thickness of the foils (around 1%) and the uncertainty on the recommended cross section (around 10%). The contribution of the irradiation time is not significant and has been neglected.

2.3. Comparison with the TALYS 1.6 code

In this work, all the experimental cross section values are compared with the latest version (1.6) of the TALYS code released in December, 2013 (Koning and Rochman 2012). TALYS is a nuclear reaction program to simulate the reaction induced by light particles on nuclei heavier than carbon. It incorporates many theoretical models to predict observables including theoretical cross section values as a function of the incident particle energy (from 1 keV to 1 GeV). Parameters are associated to these models in the input file. A combination of parameters that better describe the whole set of data available for all projectiles, targets and incident energies has been defined by the authors and put as default in the code. However, when looking to specific types of reaction, like deuteron-induced reaction, in a specific energy range (between 1–70 MeV) and for specific observables, another set of parameters, related to theoretical models, may give better results. In this work, we obtained a new combination of parameters, using newer models included in the code and plotted as TALYS Adj. in the graphs. The combined parameters presented below are the same for protons and deuterons and have shown a good reproducibility for different targets : the optical potential of Han *et al* (2006) (only for deuterons because there is only one validated model for protons), the exciton model for pre-equilibrium reaction, numerical transition rates with an optical model for collision probability and the microscopic level densities (Skyrme force) from Hilaire's combinatorial tables (Koning and Rochman 2012). The experimental data obtained in this work are compared to TALYS with default parameters (named TALYS 1.6 Default) and with these 'combined' parameters (named TALYS 1.6 Adj.). This will help the code developers to look in different directions and particularly at the newest models available.

3. Results and discussions

New production cross section for the reactions $^{232}\text{Th}(p,x)$ and $^{232}\text{Th}(d,x)$ have been obtained during our experiments and this paper focuses on the radioisotopes of medical interest produced in the target. These new data are plotted as full circles in figures 1–6 and compared with the published experimental values (EXFOR database, National Nuclear Data Center) where available and with the results obtained with the latest version of the TALYS code (plotted as dotted lines for default parameters and as dashed lines for 'combined' parameters).

3.1. Activation products

The irradiation of a thorium target by light charged particles allows the production of the mother nuclei of three promising alpha emitters for targeted therapy and will allow us to make generator systems : Thorium-227/Radium-223, Actinium-225/Bismuth-213 and Protactinium-230/Thorium-226. The production cross section of the parent radio-nuclides are plotted and discussed in this section and the numerical values are listed in tables 4 and 5.

Table 4. Experimental cross section values (mbarn) for the $^{232}\text{Th}(\text{p},\text{x})^{230}\text{Pa}$, ^{227}Th and ^{225}Ac reactions.

Energy (MeV)	$\sigma^{230}\text{Pa}$ (mb)	$\sigma^{227}\text{Th}$ (mb)	$\sigma^{225}\text{Ac}$ (mb)
17.81 \pm 1.18	104.60 \pm 13.93		
20.08 \pm 1.07	311.85 \pm 41.59		
25.53 \pm 0.79	175.01 \pm 23.48		
30.19 \pm 0.56	67.11 \pm 8.88		
36.92 \pm 0.93	38.15 \pm 5.12		
41.06 \pm 0.79	33.71 \pm 4.53		1.09 \pm 0.73
45.92 \pm 0.56	27.39 \pm 3.70	8.31 \pm 1.39	4.14 \pm 0.81
57.68 \pm 1.03	20.00 \pm 2.97	35.22 \pm 4.99	7.23 \pm 1.54
70.12 \pm 0.53	14.35 \pm 2.12	47.63 \pm 5.66	6.13 \pm 1.52

Table 5. Experimental cross section values (mbarn) for the $^{232}\text{Th}(\text{d},\text{xn})^{230}\text{Pa}$ reaction.

Energy (MeV)	$\sigma^{230}\text{Pa}$ (mb)
16.60 \pm 0.69	0.91 \pm 0.23
19.61 \pm 0.39	7.18 \pm 1.16
21.47 \pm 0.32	56.22 \pm 8.60
22.98 \pm 0.46	235.50 \pm 35.49
23.43 \pm 0.52	251.86 \pm 37.81
25.23 \pm 0.45	296.05 \pm 45.13
26.74 \pm 0.51	263.19 \pm 40.04
27.79 \pm 0.33	235.44 \pm 36.75
28.33 \pm 0.38	203.23 \pm 30.53
29.88 \pm 0.32	151.86 \pm 22.81
31.00 \pm 0.39	139.12 \pm 21.53
32.00 \pm 0.37	116.45 \pm 17.98
33.10 \pm 0.32	104.43 \pm 16.28

3.1.1. Production of ^{225}Ac .

The ^{225}Ac ($T_{1/2} = 10.1$ (1) d)/ ^{213}Bi ($T_{1/2} = 45.59$ (6) min) generator has shown its therapeutic efficacy for the targeted alpha therapy of cancer (Morgenstern *et al* 2012). ^{225}Ac can be produced in a cyclotron using a thorium target and protons with energies higher than 40 MeV (Engle *et al* 2014). However, up to 80 MeV, the ^{225}Ac production cross section is small. Its production will be interesting only with accelerators able to deliver protons with an energy higher than 100 MeV (Los Alamos National Laboratory, Brookhaven National Laboratory, The Institute for Nuclear Research in Russia). Since the threshold of the reaction $^{232}\text{Th}(\text{p},2\text{p}6\text{n})^{225}\text{Ac}$ is 42.089 MeV, this work only permits us to obtain four data points for the ^{225}Ac production cross section using protons as projectiles. No data have been obtained using deuterons as projectiles as the threshold of the $^{232}\text{Th}(\text{d},2\text{p}7\text{n})^{225}\text{Ac}$ reaction is 44.514 MeV, well above the energy available with ARRONAX.

The production cross section using protons as projectiles is plotted as full circles in figure 1. The experimental data are compared with the literature and the last version of the TALYS code, using default parameters (TALYS 1.6 Default) and combined parameters (TALYS 1.6 Adj.). The results of this work are in good agreement with Ermolaev *et al* (2012), only from 45 MeV as, in our case, no ^{225}Ac has been detected below 40 MeV. Our points showed the same trend as the one published by Gauvin (1963) and Weidner *et al* (2012), but with higher

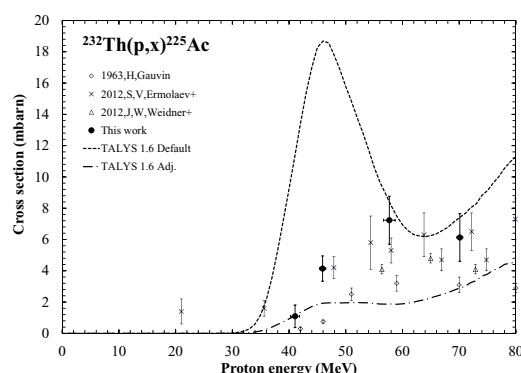


Figure 1. $^{232}\text{Th}(\text{p},\text{x})^{225}\text{Ac}$ production cross section.

values. The TALYS code using default parameters doesn't reproduce the trend and the amplitude of the experimental cross section. A better result can be obtained using the combined parameters even if the trend is not well reproduced.

3.1.2. Production of ^{227}Th .

^{227}Th has a half-life of 18.72 (2) d and decays by emitting an alpha particle to the radioisotope of medical interest ^{223}Ra ($T_{1/2} = 11.435$ (4) d). Since May 2013, the radiopharmaceutical Radium-223 dichloride (Harrison *et al* 2013), has been approved by the US Food and Drug Administration (FDA). It is marketed as 'Xofigo' by Bayer HealthCare Pharmaceuticals Inc. (Pazdur and Keegan, 2013) for the treatment of patients with castration-resistant prostate cancer which spreads as bone metastases.

As well as for ^{225}Ac , the production of ^{227}Th is only possible at high energy above 30.848 MeV which corresponds to the threshold of the $^{232}\text{Th}(\text{p},\text{p}5\text{n})^{227}\text{Th}$ reaction. In our work, the production using deuterons as projectiles is not accessible as the threshold of the reaction $^{232}\text{Th}(\text{d},\text{p}6\text{n})^{227}\text{Th}$ is 33.224 MeV, which corresponds to our upper limit. The ^{227}Th production cross section is plotted in figure 2 and compared with the literature and the TALYS code.

The results of this work are higher than those previously published (Hogan *et al* 1979, Ermolaev *et al* 2012, Weidner *et al* 2012) but follow the same trend. The data of Ermolaev *et al* and Weidner *et al* are coming from a high energy proton beam (above 100 MeV), degraded to reach the energy of interest. This may lead to a large spread of the beam energy and errors on the production cross section or/and on the referenced cross section. In the case of Hogan *et al* 1979 a chemical extraction is carried out with a yield of 65% which can induce non-negligible errors. In our case, the first thorium foil of our stack receives the energy extracted from the cyclotron. Only the second thorium foils (at 57.7 MeV), composing the stack irradiated with a proton beam of 70.3 MeV, is impinged by a degraded energy (see table 2). No chemical procedure has been carried out in our case. Moreover, looking at the logarithmic scale plot in figure 2(b), we can see that our data are in good agreement with the threshold energy for this reaction at 30 MeV (see table 3). The TALYS code with default parameters doesn't permit us to reproduce the experimental data whereas with our combined parameters considerably good results are obtained. During the irradiation, the long half-life isotope ^{228}Th ($T_{1/2} = 1.9$ years) will be produced, as shown by Ermolaev *et al* (2012). In this work, this isotope was not produced in sufficient quantity to be detected.

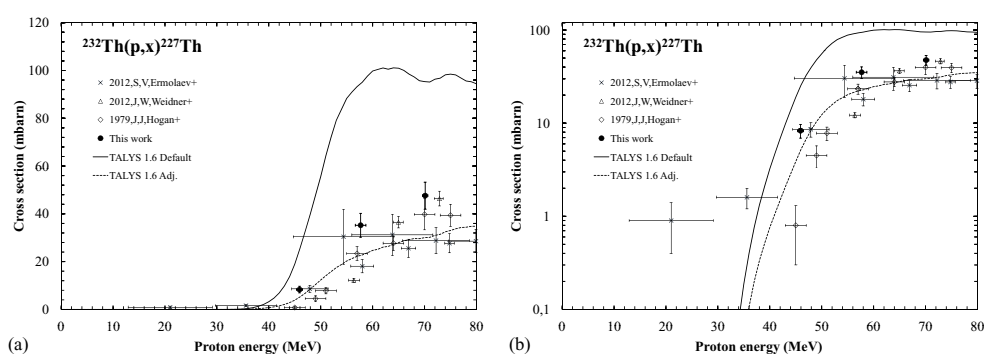


Figure 2. $^{232}\text{Th}(p,x)^{227}\text{Th}$ production cross section—linear scale (a), logarithmic scale (b).

3.1.3. Production of ^{230}Pa .

^{230}Pa with a half-life of 17.4 (5) d decays at 0.0032% by emitting an alpha particle to ^{226}Ac , 92.2 (7)% by electronic capture to ^{230}Th and at 7.8 (7)% by beta- decay to ^{230}U . ^{230}U ($T_{1/2} = 20.8$ d) decays at 100% to the medical radionuclide, ^{226}Th with a half-life of 30.57 (10) min. It is a novel therapeutic radionuclide of interest since it has been found a more potent α emitter for leukemia therapies than ^{213}Bi (Friesen *et al* 2009). The production cross sections are plotted in figures 3(a) and (b) for both projectiles: protons (a) and deuterons (b) and compared with data already published and TALYS calculations.

Using protons as projectiles (figure 3(a)), our new experimental values are in agreement with the data available on the EXFOR database and especially with the last published data set (Morgenstern *et al* 2008). Our work is consistent with the energy threshold of the $^{232}\text{Th}(p,3n)$ reaction at 13.710 MeV. The combined parameters of the TALYS code give a perfect result both in trend and values while the default parameters over-estimate the production cross section.

Using deuterons as projectiles (figure 3(b)), our new data set agrees with the energy threshold associated to $^{232}\text{Th}(d,4n)$ reaction (16.013 MeV) and shows a maximum of 296 mb at 25.23 MeV. Compared to the existing data (Rama *et al* 1986), the shape of our data set and the maximum value of the cross section are in good agreement. However, the position of the maximum is slightly shifted. In 1986, Rama Rao *et al* used energy loss values from the tables of Northcliffe *et al* (1970), which list some values for uranium but not for thorium. A bad energy estimation can lead to the use of an incorrect recommended cross section value and thus an incorrect estimation of the investigated cross section will be obtained. In addition, the branching ratio value used by Rama Rao *et al* in 1986 is different from the actual consensus (National Nuclear Data Center 0000, Ekström and Firestone 2004). Making the calculation with the older branching ratio used by Rama Rao *et al* (28%), our values increase by 5%, coming closer to the existing series of Rama Rao *et al*. The TALYS calculation using default parameters shows that neither the shape nor the maximum value of the cross section is reproduced. The combined parameters gave a good order of magnitude but shifted towards lower energies.

3.2. Fission products

Twenty-five fission products have been detected in the thorium target with an atomic mass A between 72 and 151, for both type of projectiles. Among them, three radio-isotopes are

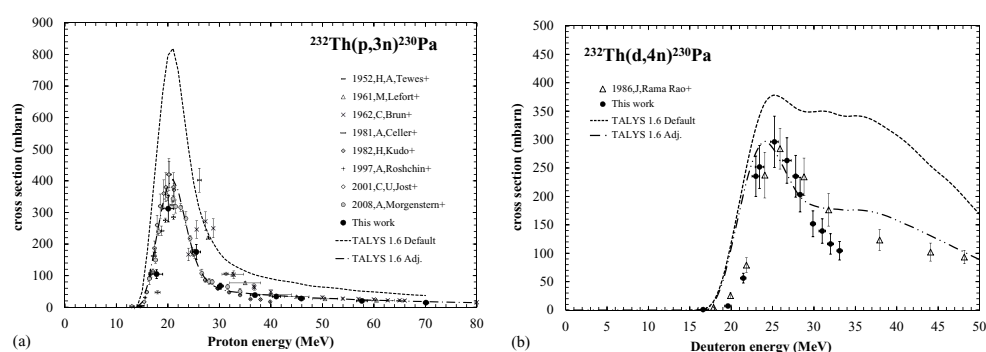


Figure 3. $^{232}\text{Th}(p,3n)^{230}\text{Pa}$ (a) and $^{232}\text{Th}(d,4n)^{230}\text{Pa}$ (b) production cross sections.

of medical interest and will be discussed in this section. The numerical values are shown in tables 6 and 7. The production cross sections presented here are cumulative cross sections as there are several hours of cooling time between the end of the irradiation and the counting measurements. In these conditions, decay occurs for short half-life isotopes. In the TALYS calculations, this phenomenon has been taken into account.

3.2.1. Production of ^{99}Mo .

^{99}Mo with a half-life of 65.94 (1) h is a β^- emitter which directly decays at 82.4% to ^{99m}Tc ($T_{1/2} = 6.01$ (1) h), the most commonly used imaging agent worldwide. The production cross sections using protons (a) and deuterons (b) as projectiles are shown in figure 4 and compared with other experimental data where available, estimated values (Abbas *et al* 2012) and the last version of the TALYS code.

The measured ^{99}Mo production cross section induced by protons (figure 4(a)) are in agreement with the value at 11.5 MeV published by Choppin and Tofe (1971) and Kudo *et al* (1982), give higher cross section values or shifted values. No discrepancies between the nuclear constants used by Kudo *et al* and in our work have been noted. However, Kudo *et al* calculated an energy loss in the uranium instead of thorium due to the lack of data for this material in the tables of Northcliffe and Schilling. As for Rama Rao *et al* this approximation could explain the discrepancies between the series.

In Abbas *et al* (2012) used Kudo *et al* data to obtain the expected production yield up to 40 MeV, adjusting the cross section values. The results of this fit are plotted in figure 4 as a full line. As our new data set is not in agreement with (Kudo *et al* 1982), it is also not in agreement with the estimation made by Abbas *et al* (2012) with a difference up to 25%. The ^{99}Mo cross section reaches a maximum around 60 MeV and decreases above this value. The TALYS code using combined parameters well reproduces the trend and the amplitude, which is not the case using the default parameters.

In figure 4(b), our work on the ^{99}Mo production induced by deuterons can only be compared with the value at 11.5 MeV of Choppin and Tofe (1971). This value is in agreement with our data set. The cross section is of the same order of magnitude and gives the same trend with protons as projectiles (figure 4(a)). As our higher energy data point with deuterons is 33.10 MeV and no data are available over this energy, it can just be proposed as an hypothesis that the cross section behavior using deuterons will be the same as for protons. The combined parameters in the TALYS code give the same trend as the experimental one except around 22 MeV and give better results than with the default parameters.

Table 6. Experimental cross section values (mbarn) for $^{232}\text{Th}(\text{p},\text{f})^{99}\text{Mo}$, $^{115\text{g}}\text{Cd}$ and ^{131}I reactions.

Energy (MeV)	$\sigma^{99}\text{Mo}$ (mb)	$\sigma^{115\text{g}}\text{Cd}$ (mb)	$\sigma^{131}\text{I}$ (mb)
11.05 ± 1.78	1.03 ± 0.09		1.10 ± 0.14
14.38 ± 1.41	6.21 ± 0.45	2.66 ± 0.19	7.30 ± 0.61
17.81 ± 1.18	17.36 ± 1.53	9.57 ± 0.86	22.16 ± 2.05
20.08 ± 1.07	24.52 ± 2.18	16.85 ± 1.51	30.52 ± 2.86
25.53 ± 0.79	32.45 ± 2.90	27.70 ± 2.51	41.37 ± 3.89
30.19 ± 0.56	37.57 ± 3.21	37.55 ± 3.34	47.06 ± 4.19
36.92 ± 0.93	40.19 ± 3.50	44.34 ± 3.98	46.89 ± 4.23
41.06 ± 0.79	44.11 ± 3.85	50.14 ± 4.52	49.04 ± 4.40
45.92 ± 0.56	44.68 ± 3.89	52.05 ± 4.68	46.60 ± 4.22
57.68 ± 1.03	48.73 ± 4.46	56.65 ± 5.34	40.36 ± 3.95
70.12 ± 0.53	38.40 ± 2.54	44.83 ± 3.15	28.89 ± 2.19

Table 7. Experimental cross section values (mbarn) for $^{232}\text{Th}(\text{d},\text{f})^{99}\text{Mo}$, $^{115\text{g}}\text{Cd}$ and ^{131}I reactions.

Energy (MeV)	$\sigma^{99}\text{Mo}$ (mb)	$\sigma^{115\text{g}}\text{Cd}$ (mb)	$\sigma^{131}\text{I}$ (mb)
8.73 ± 1.14	0.32 ± 0.04	0.10 ± 0.01	0.33 ± 0.05
11.79 ± 0.93	4.43 ± 0.50	1.84 ± 0.21	4.92 ± 0.56
14.33 ± 0.81	11.98 ± 1.31	5.46 ± 0.60	13.05 ± 1.54
16.60 ± 0.69	16.72 ± 1.84	9.16 ± 1.02	18.76 ± 2.18
19.61 ± 0.39	19.89 ± 2.50	12.04 ± 1.52	22.54 ± 2.86
21.47 ± 0.32	23.17 ± 2.73	15.06 ± 1.80	26.78 ± 3.19
22.98 ± 0.46	32.75 ± 3.77	22.55 ± 2.63	39.81 ± 4.90
23.43 ± 0.52	34.31 ± 3.91	26.21 ± 3.01	35.34 ± 4.11
25.23 ± 0.45	38.70 ± 4.55	30.22 ± 3.56	43.80 ± 5.27
26.74 ± 0.51	36.22 ± 4.26	29.05 ± 3.45	41.83 ± 4.98
27.79 ± 0.33	41.18 ± 5.01	34.71 ± 4.23	48.78 ± 6.35
28.33 ± 0.38	41.07 ± 4.71	33.97 ± 3.92	48.46 ± 5.66
29.88 ± 0.32	40.48 ± 4.63	33.32 ± 3.84	47.41 ± 5.53
31.00 ± 0.39	38.56 ± 4.64	30.12 ± 3.66	44.13 ± 5.35
32.00 ± 0.37	38.26 ± 4.58	32.88 ± 3.96	44.36 ± 5.37
33.10 ± 0.32	40.20 ± 4.89	35.11 ± 4.29	46.34 ± 5.70

3.2.2. Production of $^{115\text{g}}\text{Cd}$.

In the literature, a method has been proposed (Ehrhardt *et al* 1983) to obtain $^{115\text{m}}\text{In}$ with high yield and high purity. This radioisotope has the potential for medical imaging due to its appropriate half-life and since the behavior of its radioisotope ^{111}In for labeling blood has already been studied. In our thorium targets, $^{115\text{m}}\text{In}$ is obtained via the production of its mother nuclei $^{115\text{g}}\text{Cd}$. ^{115}Cd has a metastable state, $^{115\text{m}}\text{Cd}$, with a half-life of 44.6 (3) d and a ground state, $^{115\text{g}}\text{Cd}$, with a half-life of 53.46 (10) h. $^{115\text{g}}\text{Cd}$ decays by β^- emission at 100% to the metastable state $^{115\text{m}}\text{In}$ ($T_{1/2} = 4.486$ (4) h). New data on the $^{115\text{g}}\text{Cd}$ cross sections are shown in figures 5(a) and (b) for protons and deuterons as projectiles, respectively.

Using protons as projectiles, $^{115\text{g}}\text{Cd}$ shows a higher production cross section than ^{99}Mo but the same shape with an increase of up to 60 MeV and a decrease above this energy value. An energy shift always exists between our data and those published by Kudo *et al* (1982), for the same reason as the one proposed for the ^{99}Mo production. The study involving deuterons

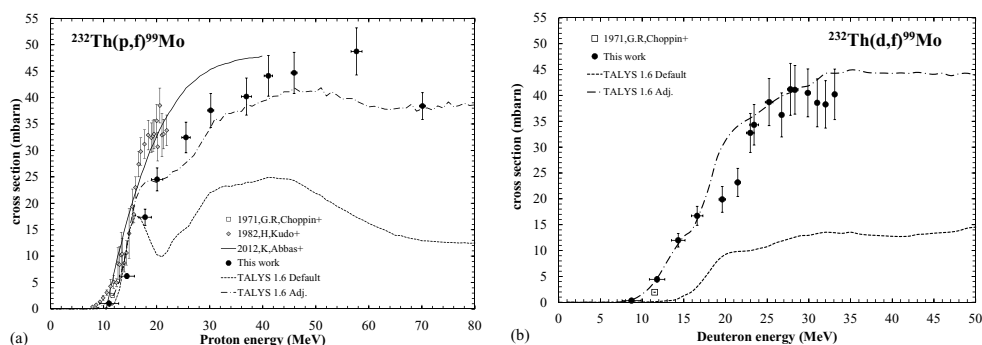


Figure 4. $^{232}\text{Th}(p,f)^{99}\text{Mo}$ (a) and $^{232}\text{Th}(d,f)^{99}\text{Mo}$ (b) production cross sections.

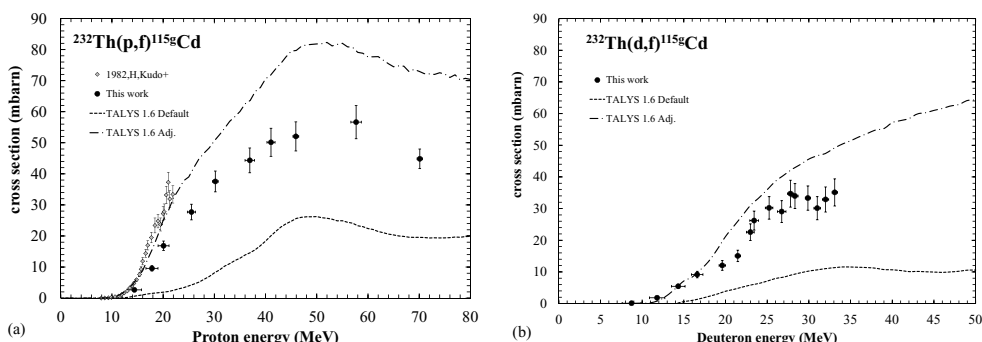


Figure 5. $^{232}\text{Th}(p,f)^{115g}\text{Cd}$ (a) and $^{232}\text{Th}(d,f)^{115g}\text{Cd}$ (b) production cross sections.

as projectiles plotted in figure 5(b) is the first data set available up to 33.1 MeV. The values are of the same order of magnitude as those obtained with protons. In both cases, protons or deuterons, the combined parameters of the TALYS code over-estimates the data while using the default parameters, data are under-estimated.

3.2.3. Production of ^{131}I .

^{131}I commonly called 'radioactive iodine' has been used since the 1940s in the therapy of diseases related to the thyroid (Mumtaz *et al* 2009). This radioisotope, with a half-life of 8.02070 (11) d, is a β^- emitter administered as an oral dose as a substitute for the natural iodine present in the human body, to kill the thyroid cells. Linked with a monoclonal antibody, ^{131}I is also used in the treatment of certain types of Non-Hodgkin's lymphomas (Vose 2004). A new set of data for the production of ^{131}I using thorium target and particles available on cyclotrons are shown in figure 6.

In figure 6(a), the ^{131}I cumulative production cross section, obtained after the total decay of ^{131}Te , shows a maximum of 50 mbarn at 41 MeV. In this case, the decrease of the cross section appears at lower energy (around 45 MeV) than for ^{99}Mo and ^{115g}Cd . With deuterons, the cross section (see figure 6(b)) is still increasing at 33.1 MeV and has a similar magnitude to protons. The value published at 11.5 MeV by Freid *et al* (1968) is closer to our points than the one obtained at the same energy by Choppin and Tofe (1971). The TALYS code used with combined parameters is able to reproduce the experimental data for protons and deuterons as projectiles which is not the case with the default parameters.

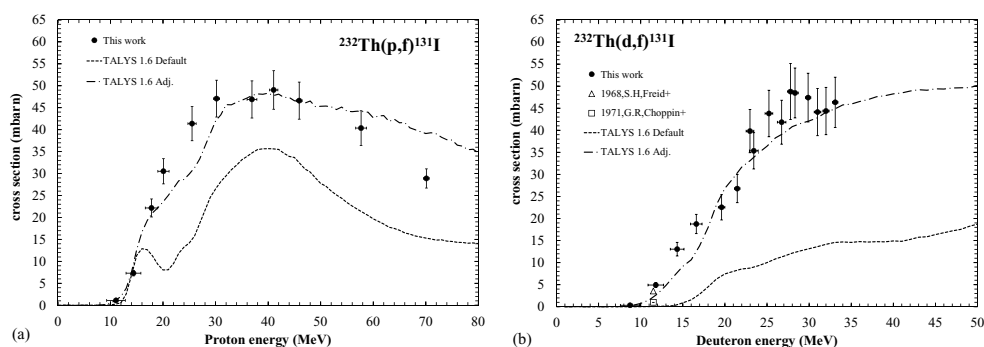


Figure 6. $^{232}\text{Th}(p,f)^{131}\text{I}$ (a) and $^{232}\text{Th}(d,f)^{131}\text{I}$ (b) production cross sections.

3.3. Thick target yield (TTY)

Using all the cross section values obtained in this work, we have calculated for each radionuclide produced, its thick target yield (TTY) in MBq/ $\mu\text{A}\cdot\text{h}$ as a function of the projectile energy, using the formula (1).

$$\text{TTY} = \Phi \cdot \chi \cdot \frac{N_a \cdot \rho}{A} (1 - e^{-\lambda \cdot t}) \int_{E_{\min}}^{E_{\max}} \frac{\sigma(E)}{\frac{dE}{dx}} dE \quad (1)$$

Where χ is the target enrichment and dE/dx is the specific energy loss of the projectile in the target material ($\text{MeV}\cdot\text{cm}^{-1}$). In a thick target, the incident particle energy decreases with the penetration depth. E_{\max} corresponds to the incident projectile energy when it enters into the target whereas E_{\min} corresponds to its energy when it leaves the target. The thick target yield can also be called production yield or integral yield. The thick target yields of the activation products and fission products are plotted in figure 7. The production of these radionuclides is calculated at the end of irradiation, except for ^{230}U and ^{223}Ra . In these cases, the radio-isotopes are obtained by the decay of their parents produced in the target, ^{230}Pa and ^{227}Th respectively. We choose to show values corresponding to the case where only one chemical recovery process is performed at the time when their activity is at maximum. For the activation products plotted in figure 7(a), the maximum ^{230}U activity is obtained using protons as projectiles. For ^{223}Ra and ^{227}Th , we can't compare both production routes as we were not able to obtain data using deuterons and no data are available in the literature.

For the fission products' plot in figure 7(b), the deuteron routes are drawn as crosses and the proton routes as full lines. This plot shows that the proton route is preferred.

In table 8 are listed the medical isotopes produced on a thorium target irradiated with a cyclotron able to deliver protons with a maximal energy of 70 MeV and a maximal intensity of 350 μA .

This way, the activity values are obtained after an irradiation time of 3 d (taking into account the ^{99}Mo half-life) with an intensity of 350 μA and the hypothesis of a dedicated accelerator with 90 productions per year. A large amount can be produced, as seen in table 8. For the sake of completeness, the maximum patient dose considered for an alpha emitter is around 10 mCi, between 40 and 300 mCi for β^- emitters as ^{131}I (Aubert and Chatal 2006) and between 10 and 30 mCi for ^{99m}Tc (Mallinckrodt Pharmaceuticals 2014). A $^{99}\text{Mo}/^{99m}\text{Tc}$ generator system contains around 3 Ci of ^{99}Mo when it's received by a hospital. In the United States of America, most nuclear medical clinics received a 10 Ci $^{99}\text{Mo}/^{99m}\text{Tc}$ generator each week.

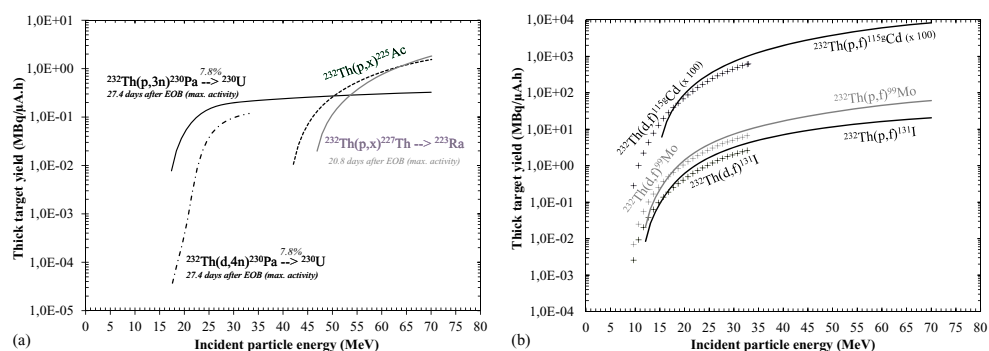


Figure 7. Production yields of the activation (a) and fission products (b).

Table 8. Medical isotopes on a ^{232}Th target irradiated by protons of 70 MeV.

Radioisotope	Half-life $T_{1/2}$	TTY at 70 MeV (MBq/μA.h)	Prod. 350 μA during 3 d (Ci)	Prod. on a dedicated machine at 70 MeV: 90 prod./year (Ci)
^{230}U	20.8 d	0.3 (after 27.4 d)	0.2	18
^{225}Ac	10.0 d	1.6	1.1	99
^{223}Ra	11.435 d	1.8 (after 20.8 d)	1.2	108
^{131}I	8.0207 d	20.6	14.0	1 260
^{115}gCd	53.46 h	83.1	56.6	5 094
^{99}Mo	65.94 h	61.1	41.6	3 744

3.3.1. Focus on ^{99}Mo production.

In this part we focus our study on the production of ^{99}Mo . As explained in the introduction, the NEA Steering Committee for Nuclear Energy requested a review of other potential methods for the production of $^{99}\text{Mo}/^{99m}\text{Tc}$ using reactors or accelerators (NEA 2010). Within this framework, we have compared the production of ^{99}Mo using different production routes accessible with cyclotrons. These values, summarized in table 9, are calculated with the parameters of a commercial 70 MeV cyclotron (as an example; the ARRONAX cyclotron) delivering a maximal intensity of 350 μA for protons with a maximum incident energy of 70 MeV, 50 μA for deuterons of 35 MeV and 70 μA for alphas of 68 MeV.

The higher yield is obtained using protons and a 100% enriched ^{100}Mo target. But in this case, the specific activity will be very different to what is actually used. In order to get high specific activity it is possible to use proton-induced reaction on ^{232}Th and $^{\text{nat}}\text{U}$. The irradiation of uranium gives higher ^{99}Mo yield than the irradiation of thorium but it leads to the production of long half-life radionuclides like ^{237}Np ($2 \cdot 10^6$ years), ^{236}Np ($1.5 \cdot 10^5$ years) and ^{236}U ($2.3 \cdot 10^7$ years), which are not produced in a thorium target. Moreover, thorium is three times more abundant in nature than uranium (IAEA *et al* 2005) which makes it less expensive. The fission of thorium, either induced by neutrons or light charged particles, can be used to produce high specific activity ^{99}Mo .

4. Conclusion

New cross section data on the production of medical radioisotopes using a thorium target irradiated by light charged particles are reported in this work.

Table 9. Comparison of different ^{99}Mo production routes.

Reaction	Author	Energy (MeV)	TTY (MBq/ $\mu\text{A.h}$)	Prod. during 3 d (Ci)	Prod. on a dedicated machine with 90 prod./year (Ci)
$^{100}\text{Mo}(\text{p,pn})$	Tárkányi et al (2012)	38	98.8	67.3	6 057
$^{\text{nat}}\text{U}(\text{p,f})$	Uosif et al (2005)	70	80.4	54.8	4 932
$^{232}\text{Th}(\text{p,f})$	This work (2014)	70	61.1	41.6	3 744
$^{\text{nat}}\text{Pb}(\text{p,f})$	Kuhnhen et al (2001)	70	1.3	0.9	81
$^{100}\text{Mo}(\text{d,p}2\text{n})$	Tárkányi et al (2011)	35	76.0	7.4	666
$^{232}\text{Th}(\text{d,f})$	This work (2014)	33	6.7	0.7	63
$^{100}\text{Mo}(\alpha, \text{an})$	Levkovskij (1991)	46	2.0	0.3	25
$^{96}\text{Zr}(\alpha, \text{n})$	Pupillo et al (2014)	30	1.6	0.2	18

Some comparisons have been made with the results of the latest version of the TALYS code showing that the default parameters defined for this code are not always able to reproduce the experimental data. However, other models included in the code are better able to describe our set of data. In this work, we obtained a robust set of parameters which better reproduce the data than the default parameters for protons and deuterons as projectiles and for targets with an atomic mass from 46 to 232.

Production yields have been obtained for the ^{223}Ra and ^{225}Ac radionuclides using proton beams up to 70 MeV. The production of four other radioisotopes for medical use has been compared in the case of protons or deuterons as projectiles : $^{230}\text{Pa}/^{230}\text{U}$, ^{99}Mo , ^{115}gCd and ^{131}I . In each case, the proton route is preferred. ^{99}Mo production has been compared in the case of different targets and projectiles. The route using protons and a 100% enriched ^{100}Mo target will give the higher yield using a dedicated cyclotron. But in this case, the specific activity will not reach the current used value. Another way to reach high activity products is to use a uranium target but the activation will lead to the production of neptunium radioisotopes with long half-life. The irradiation of a thorium target by protons can be an alternative.

Acknowledgments

The ARRONAX cyclotron is a project promoted by the Regional Council of Pays de la Loire financed by local authorities, the French government and the European Union. This work has been, in part, supported by a grant from the French National Agency for Research called ‘Investissements d’Avenir’, Equipex Arronax-Plus n° ANR-11-EQPX-0004 and Labex n° ANR-11-LABX-0018-01.

References

- Abbas K, Holzwarth U, Simonelli F, Kozempel J, Cydzik I, Bulgheroni A, Cotogno G, Apostolidis C, Bruchertseifer F and Morgenstern A 2012 Feasibility of ^{99}Mo production by proton-induced fission of ^{232}Th *Nucl. Instrum. Methods Phys. Res. B* **278** 20–5
- AIPES 2008 Molybdenum-99 production for nuclear medicine 2010–2020 Report www.aipes-eeig.org and www.aipes-eeig.org/index.php?id=57
- Aubert B and Chatal J F 2006 Radiation protection for innovative diagnostic and therapeutic approaches in nuclear medicine *Radioprotection* **41** 33–50
- Blessing G, Brautigam W, Boge H G, Gad N, Scholten B and Qaim S M 1995 Internal irradiation system for excitation function measurement via the stacked-foil technique *Appl. Radiat. Isot.* **955** 46–9
- Choppin G R and Tofe A J 1971 Charged particle fission of ^{232}Th *J. Inorg. Nucl. Chem.* **33** 1535–41

- Duchemin C, Guertin A, Haddad F, Michel N and Metivier V 2015 Cross section measurements of deuteron induced nuclear reactions on natural tungsten upto 34 MeV *Appl. Radiat. Isot.* **97** 52–8
- Engle J W *et al* 2014 Ac, La and Ce radioimpurities in ²²⁵Ac produced in 40–200 MeV proton irradiations of thorium *Radiochim. Acta* **102** 569–81
- Ehrhardt G J, Volkert W, Goeckeler W F and Kapsch D N 1983 A new Cd-115 → In-115m radionuclide generator *J. Nucl. Med.* **24** 349–52
- Ekström L F and Firestone R B 2004 Information extracted from the table of radioactive isotopes, version 2.1
- Ermolaev S V, Zhuikov B L, Kokhanyuk V M, Matushko V L, Kalmykov S N, Aliev R A, Tananaev I G and Myasoedov B F 2012 Production of actinium, thorium and radium isotopes from natural thorium irradiated with protons up to 141 MeV *Radiochim. Acta* **100** 223–9
- FitzPeaks Gamma Analysis and Calibration Software Version 3.66 1981 produced by JF computing services (UK), based on methods presented *Nucl. Instrum. Methods* **190** 89–99 (describing the program SAMPO80 of the Helsinki University of Technology, Finland)
- Freid S H, Anderson J L and Choppin G R 1968 Charged distribution in the fission of ²³²Th *J. Inorg. Nucl. Chem.* **30** 3155–65
- Friesen C, Roscher M, Morgenstern A, Bruchertseifer F, Abbas K and Apostolidis C 2009 Radioimmunotherapy using anti-CD33 antibodies radiolabeled with thorium-226 or bismuth-213 overcome chemo- and radioresistance in myeloid leukemia cells *Haematologica* **94** 32
- Gauvin H 1963 Reactions(p,2p alpha n) sur le thorium 232 de 30 a 120 MeV *J. Phys.* **24** 836–8
- Haddad F, Ferrer L, Guertin A, Carlier T, Michel N, Barbet J and Chatal J F 2008 Arronax a high-energy and high-intensity cyclotron for nuclear medicine *Eur. J. Nucl. Med. Mol. Imaging* **35** 1377–87
- Han Y, Shi Y and Shen Q 2006 Deuteron global optical model potential for energies up to 200 MeV *Phys. Rev. C* **74** 044615
- Harrison M R, Wong T Z, Armstrong A J and George D J 2013 Radium-223 chloride: a potential new treatment for castration-resistant prostate cancer patients with metastatic bone disease *Cancer Manag. Res.* **5** 1–4
- Hogan J J, Gadioli E, Gadioli-Erba E and Chung C 1979 Fissionability of nuclides in the thorium region at excitation energies to 100 MeV *Phys. Rev. C* **20** 1831
- International Atomic Energy Agency 2005 Thorium fuel cycle—potential benefit and challenges IAEA-TECDOC-1450
- Koning A J and Rochman D 2012 Modern nuclear data evaluation with the TALYS code system *Nucl. Data Sheets* **113** 2841
- Kudo H, Muramatsu H, Nakahara H, Miyano K and Kohno I 1982 Fission fragment yields in the fission of ²³²Th by protons of energies 8 to 22 MeV *Phys. Rev. C* **25** 3011–23
- Kuhnenn J, Herpers U, Glasser W, Michel R, Kubik P W and Suter M 2001 Thin target cross sections for proton-induced formation of radionuclides from lead for $E_p \leq 71$ MeV *Radiochim. Acta* **89** 697–702
- Levkovskij V N 1991 Activation cross section nuclides of average masses ($A = 40$ – 100) by protons and alpha-particles with average energies ($E = 10$ – 50 MeV) *Activation Cross Section by Protons and Alphas* (Moscow)
- Mallinckrodt Pharmaceuticals 2014 *Kit for the Preparation of Technetium Tc 99m Sestamibi Injection* (www.mallinckrodt.com)
- Michel R *et al* 1997 Cross sections for the production of residual nuclides by low- and medium-energy protons from the target elements C, N, O, Mg, Al, Si, Ca, Ti, V, Mn, Fe, Co, Ni, Cu, Sr, Y, Zr, Nb, Ba and Au *Nucl. Instrum. Methods B* **129** 153
- Morgenstern A, Apostolidis C, Bruchertseifer F, Capote R, Gouder T, Simonelli F, Sin M and Abbas K 2008 Cross-sections of the reaction ²³²Th(p,3n)²³⁰Pa for production of ²³⁰U for targeted alpha therapy *Appl. Radiat. Isot.* **66** 1275–80
- Morgenstern A, Bruchertseifer F and Apostolidis C 2012 Bismuth-213 and Actinium-225 Generator performance and evolving therapeutic applications of two generator-derived alpha-emitting radioisotopes *Curr. Radiopharmaceuticals* **5** 221–7
- Mumtaz M, Shueh Lin L, Chong Hui K and Sharifuddin M K A 2009 Radioiodine I-131 for the therapy Of grave disease, special communication *Malaysian J. Med. Sci.* **16** 1
- National Nuclear Data Center, information extracted from the NuDat2 database and www.nndc.bnl.gov/nudat2/
- Northcliffe L C and Schilling R R 1970 *Nucl. Data Tables A* **7** 233

- Nuclear Energy Agency (NEA) 2010 Organisation for economic co-operation and development (OECD) 2010 The supply of medical radioisotopes: review of potential molybdenum-99/technetium-99m production technologies
- Pazdur R and Keegan P 2013 FDA approval for radium 223 Dichloride, FDA article
- Pupillo G, Esposito J, Gambaccini M, Haddad F and Michel N 2014 Experimental cross section evaluation for innovative ^{99}Mo production via the (a,n) reaction on ^{96}Zr target *J. Radioanal. Nucl. Chem.* **302** 911–7
- Rama R J, Ernst J and Machner H 1986 Comparative study of d- and ^6Li - induced reactions on ^{232}Th in terms of breakup and preequilibrium processes *Nucl. Phys. A* **448** 365–80
- Tárkányi F, Ditrói F, Hermanne A, Takács S and Ignatyuk A V 2012 Investigation of activation cross-sections of proton induced nuclear reactions on natMo up to 40 MeV: new data and evaluation *Nucl. Instrum. Methods Phys. Res. B* **280** 45–73
- Tárkányi F, Hermanne A, Takács S, Sonck M, Szucs Z, Király B and Ignatyuk A V 2011 Investigation of alternative production routes of $^{99\text{m}}\text{Tc}$: deuteron induced reactions on ^{100}Mo *Appl. Radiat. Isot.* **69** 18–25
- Takács S, Tárkányi F, Sonck M and Hermanne A 2002 New cross sections and intercomparison of proton monitor reactions on Ti, Ni and Cu *Nucl. Instrum. Methods* **188** 106
- Tárkányi F, Szelecsnyi F and Kopecky P 1991 Excitation functions of proton induced nuclear reactions on natural nickel for monitoring beam energy and intensity *Appl. Radiat. Isot.* **42** 513
- Uosif M A M, Michel R, Herpers U, Kubik P W, Duijvestijn M and Koning A 2005 Residual nuclide production by proton-induced reactions on uranium for energies between 20 and 70 MeV *Int. Conf. on Nuclear Data for Science and Technology (Santa Fe, New Mexico, USA, 26 September–1 October 2004) (AIP Conf. Proc. vol 769)* pp 1547–50
- Vose J M 2004 Bexxar[®], novel radioimmunotherapy for the treatment of low-grade and transformed low-grade non-Hodgkin's lymphoma *Oncologist* **9** 160–72
- Weidner J W et al 2012 Proton-induced cross sections relevant to production of ^{225}Ac and ^{223}Ra in natural thorium targets below 200 MeV *Appl. Radiat. Isot.* **70** 2602–7
- Ziegler J F, Ziegler M D and Biersack J P 2010 SRIM The stopping and range of ions in matter *Nucl. Instrum. Methods Phys. Res. B* **268** 1818–23
- Zalutsky M R, Garg P K, Friedman H S and Bigner D D 1989 Labeling monoclonal antibodies and F(ab')₂ fragments with the alpha-particle-emitting nuclide astatine-211: preservation of immunoreactivity and *in vivo* localizing capacity *Proc. Natl Acad. Sci. USA* **86** 7149–53